doi **https://doi.org/10.34172/bi.2023.27758**

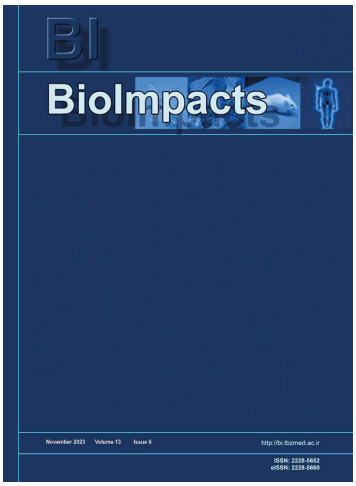

Inhibitory effect of miR342 on the progression of triple-negative breast cancer cells in vitro and in the mice model

Zahra Alidoost, Farnoosh Attari*, Fatemeh Saadatpour, Ehsan Arefian

Please cite this article as: Alidoost Z, Attari F, Saadatpour F, Arefian E. Inhibitory effect of miR342 on the progression of triple-negative breast cancer cells in vitro and in the mice model. *Bioimpacts* **2023**. doi: 10.34172/bi.2023.27758

Inhibitory effect of miR342 on the progression of triple-negative breast cancer cells *in vitro* and in the mice model

Running title: miR342 inhibits progression of breast cancer

Zahra Alidoost[1], Farnoosh Attari[1*], Fatemeh Saadatpour[2], Ehsan Arefian[2]

[1] Department of Animal Biology, School of Biology, College of Science, University of Tehran, Tehran, Iran
[2] Molecular Virology Lab, Department of Microbiology, School of Biology, College of Science, University of Tehran, Tehran, Iran

***Correspondence**
Farnoosh Attari, PhD., Assistant Professor
E-mail: Attari@ut.ac.ir, **Tel**: +9821-61112626, **Fax**: (+9821)-66405141, **Orchid:** 0000-0001-8964-2293

Zahra Alidoost Orchid**:** 0000000260513727

Abstract

Introduction: Breast cancer is the most common cancer in women worldwide, and the triple-negative subtype is the most invasive, with limited therapeutic options. Since miRNAs are involved in many cellular processes, they harbor great value for cancer treatment. Therefore, in this study, we have investigated the anti-proliferative and anti-invasive roles of miR342 in 4T1 triple-negative cells *in vitro* and also studied the effect of this miRNA on tumor progression and the expression of its target genes *in vivo*. Methods: 4T1 cells were transduced with conditioned media of miR342-transfected Hek-LentiX cells. MTT and clonogenic assays were used to assess the viability and colony-forming ability of 4T1 cells. Apoptosis and invasion rates were respectively evaluated by annexin/7-AAD and wound healing assays. At last, *in vivo* tumor progression was evaluated using H&E staining, Real-time PCR, and immunohistochemistry. Results: The viability of transduced-4T1 cells reduced significantly 48 hours after cell seeding and colony forming ability of these cells reduced to 50% of the control group. Also, miR342 imposed apoptotic and anti-invasive influence on these cells *in vitro*. A 30-day follow-up of the breast tumor in the mice model certified significant growth suppression along with reduced mitotic index and tumor grade in the treatment group. Moreover, decreased expression of Bcl2l1, Mcl1, and ID4, as miR342 target genes, was observed, accompanied by reduced expression of

VEGF and Bcl2/Bax ratio at the protein level. Conclusions: To conclude, our data support the idea that miR342 might be a potential therapeutic target for the treatment of TNBC.

Keywords: Triple-negative breast cancer, miR342, Tumor progression, Proliferation, Invasion

Introduction

Breast cancer is the most common cancer in women worldwide, generally categorized based on the expression of estrogen receptor (ER), progesterone receptor (PR), and HER2 receptor. The ER/PR/HER2 negative one, the triple-negative subtype, is highly heterogenous and accounts for the most invasive breast cancer with high metastasis ability and poor prognosis.[1] Unlike the other subtypes of breast cancer, including the hormone-responsive and HER2-positive ones, the therapy options are minimal for triple-negative breast cancer (TNBC).[2] Chemotherapy is the only efficient option for treating TNBC; however, chemoresistance occurs after initial chemosensitivity.[3] Therefore, attention was attracted to targeted treatment and gene therapy as a new therapeutic approach for TNBC. It is well-accepted that in many types of cancers, the expression of miRNAs is highly dysregulated. miRNAs are small noncoding RNAs with 19-24 nucleotides that negatively regulate their target gene via attaching to the 3'UTR of a complementary mRNA. Since miRNAs are involved in many cellular processes, including proliferation, apoptosis, and metastasis, they harbor great value in being used for cancer diagnosis and treatment. Antagomirs are used to repress aberrantly upregulated miRNAs, and miRNA mimics, with the name miRNA replacement therapy, are the way to restore the expression of the ones with loss of function.[4]

So far, many studies have employed miRNA mimics to induce apoptosis and reduce cell proliferation and invasion in TNBCs *in vitro* or *in vivo*. For example, a previous study proved the antitumor activity of miR34a on TNBC with the suppressing effect on Bcl2 expression.[5] Moreover, the role of miR598 in the repression of TNBC was triggered via targeting JAG1.[6] It was demonstrated that intravenous injection of miR206 robustly reduced the mass of xenograft tumors of TNBC.[7] In addition, eight weeks after transplantation of TNBC cells transfected with miR355 to nude mice, slower tumor growth compared to the control group was detected.[8] All of these studies highlight the importance of miRNAs as the therapeutic targets for treating TNBCs. In our research, we have focused on the role of miR342 in the growth of mice TNBC cells. miR342 was demonstrated to induce apoptosis and reduce cell proliferation of hepatocellular cancer cells by targeting Wnt/β catenin pathway.[9] Further, the tumor-suppressive role of miR342 in lung cancer was confirmed with intratumoral injection of miRNA mimics.[10]

High expression of miR342 was reported to sensitize human TNBC to chemotherapy.[11] Also, miR342 was shown to inhibit the proliferation and migration of human breast cancer cells *in vitro* via the suppression of its target genes, cofilin 1 and MTC1.[12,13] However, these data in TNBC were just verified *in vitro* and none of these studies examined the therapeutic effect of overexpression of miR342 on TNBC in the animal model and in the body condition. Therefore, in this study, we have investigated the anti-proliferative and anti-invasive roles of miR342 in the 4T1 TNBC mice cell line *in vitro* and more importantly studied the therapeutic effect of this miRNA on the tumor progression and the expression of its target genes in the mice model. To

our knowledge, this is the first study investigating the tumor-suppressing effect of this miRNA on TNBC in the mice model.

Materials and methods

Cell culture

Mice 4T1 breast cancer cell line was cultured in RPMI 1640 (Gibco, USA), and human embryonic kidney 293 T (HEK 293T) was obtained from the Iranian biological resource center (IBRC, Tehran, Iran) and cultured in Dulbecco's modified eagle's medium (DMEM) (Gibco, USA). The culture media of both cell lines were supplemented with 10% fetal bovine serum (FBS) (Gibco, Brazil) and 1% penicillin/streptomycin (Sigma, USA). The cells were grown to 80% confluence in a humidified atmosphere of 5% CO_2 at 37 °C.

Virus production and stable cell line generation

All lentivectors were obtained from the stem cell technology research center (Tehran, Iran). Lentiviruses were produced by the three-plasmid system and transient cotransfection of HEK 293T cells using polyethyleneimine (PEI MAX 40K, Polysciences) transfection reagent.[14] The mixture of the packaging helper plasmids, psPAX and pMD.2G, with miR342/scrambled recombinant pCDH-GFP-Puro lentivectors, was prepared in a total of 15 µg/ml and DNA/PEI at a 1:2 ratio. 72 hours post-transfection, lentivirus-containing supernatant was collected every 12 hours and centrifuged at 2000 × g/4 ℃ for 10 min to eliminate packaging cells collected during harvesting. The seeded 4T1 cells at a confluency of 60% were transduced with miR342/scrambled lentiviruses and examined by fluorescent microscope for GFP expression after 96 hours post-infection. The stable cells were selected using the puromycin (Sigma, USA) treatment protocol. The control and treatment groups were considered the 4T1-scramble and 4T1-miR342 stable cells.

Flow cytometry analysis

The number of 5×10^5 scramble and treated cells were seeded in a 6-well plate. Apoptosis and cell cycle alteration assays were performed after 48 hours without changing the medium. The annexin V-phosphatidylethanolamine (PE) and 7-minoactinomycin D (7-AAD) apoptosis detection kit (BD Biosciences) was used for cell apoptosis analysis based on the manufacturer's instructions. Briefly, the cell pellet was suspended in the binding buffer followed by incubation with 5 µL of annexin-PE for 10 min in the dark. After two washing steps, 5 µL of 7-AAD was added to 200 µL of suspended cells in the binding buffer. For the cell cycle assay, cells were fixed with 70% cold ethanol overnight at -20℃. Fixed cells were washed with PBS for 20 min and subjected to 50 µg/mL propidium iodide (PI; Sigma, USA), 1.0 mg/mL RNase (Thermo Fisher Scientific), and Tryton X-100 (Sigma, USA). Stained cells were incubated at 37℃ in the dark for 40 min. Apoptosis rate and sub-G1 population were measured by flow cytometry (BD Biosciences). Data were analyzed using FlowJo 7.6.1 software.

Cell viability assay

The effect of miR342 overexpression on cell viability was measured by 3-(4, 5-dimethylthiazol-2-yl)-2, 5-diphenyltetrazolium bromide (MTT, Sigma, USA) assay. Transduced 4T1 cells were seeded into 96-well plates, and then an MTT assay was performed 24, 48, 72, and 96 hours post-culture. In summary, 10 µL of MTT solution with the 5 mg/mL concentration was added to each well. After 3 hours of incubation at 37 ℃, the cell supernatant was discarded, and 100 µL DMSO was added to resolve the formazan crystals. At last, the absorbance of the obtained solution was measured at 490 nm by a microplate Elisa reader (BioTeck Elx800), and the Prism software analyzed the data.

Wound-healing and invasion assay

Wound-healing assay was used to analyze the migration ability of the 4T1 cells with stable expression of miR342-3p compared to scramble cells. 5×10^5 scramble and treated cells were seeded in a 6-well plate and were grown to 80% confluency. The monolayer was disrupted with a sterile yellow tip, washed with PBS, and incubated in 2 ml RPMI media containing 2-4% v/v FBS to stop cell proliferation. Images were taken at 0, 24, 48, and 72 hours post-injury using a phase-contrast microscope (Olympus, Tokyo, Japan). The extent of migration into the wound area was evaluated qualitatively using Image J software (NIH Image, USA). The following formulae calculated wound closure percentage (A0 = Area measured at 0 h, Ai = Area measured at 24, 48, or 72 hours): Wound closure (%) = A0 - Ai/A0 × 100

Colony formation assay

We have used a colony formation assay to assess the impact of miR342 on the proliferation ability of every single cell. In brief, about 50-100 cells were seeded in a 3 cm^2 cell culture dish. After 14 days, cells were fixed with glutaraldehyde (0.6% v/v) and stained with crystal violet (0.5 w/v). Finally, the total number of stained colonies was counted by a stereomicroscope (SUNNY, China). Also, the colony area was measured using Image J software. Cell plating efficiency was calculated as: number of colonies/number of seeded cells × 100.

In vivo tumor growth

8-weeks female BALB/c mice were used for the tumor model formation. Animals (6 mice/cage) were kept at about 22 ℃ with 12 hours of dark/light exposure with standard free access to food and water. For tumor formation, the number of 5×10^5 4T1 cells were suspended in 70 µl RPMI media and injected subcutaneously. The length and width of visible tumors were recorded daily for 30 days, and the tumor volumes were calculated as 0.5 × length × $width^2$. Also, animals were anesthetized for tumor removal using 50 mg/kg ketamine and 5 mg/kg xylazine, followed by cervical dislocation on day 30.

Hematoxylin and eosin staining

First, tumor tissues were fixed in 4% paraformaldehyde. Fixed tissues were sectioned into 5 µm slices after paraffin embedding. After deparaffinization and rehydration, tissue sections were stained with hematoxylin and eosin dyes. At last, slides were pictured using an optical microscope and were analyzed by an expert pathologist. Total tumor grade was determined based on scoring three characteristics: nuclear polymorphism, mitotic index, and glandular/tubular differentiation.

Immunohistochemistry

After deparaffinization, the sections were treated with a retrieval mixture (0.1 M sodium citrate and 0.1 M citric acid), followed by dH_2O_2 incubation. After treatment with protein block (Dako), slides were incubated with monoclonal anti-Bax (Biorbyt, USA), VEGF (Biorbyt, USA), and Bcl2 for 60 min. At last, DAB reagent (1:50, Dako) and hematoxylin dye were applied to the slides. For scoring the antibody reactivity, the modified all-red scoring system was employed in which the quick score equaled the summation of proportion score and intensity score (0–1 = negative, 2–3 = weak, 4–6 = moderate, 7–8 = strong).

Real-time PCR

miRNA and gene expression in cells and tumor tissue were evaluated using Real-time PCR. According to the manufacturer's protocol, the total RNA was extracted using RNX plus reagent (Sinacolon, Iran). The single-strand cDNA synthesis was done with an RNA template (3 µg for the synthesis of total cDNA and 1 µg for the synthesis of miRNA cDNA), random hexamer (10 µM, for total cDNA), and miRNA RT primer (1 µM, for miRNA cDNA), and reverse transcriptase (ParsTous, Iran) in a final volume of 20 µl according to thermal profiles of ParsTous cDNA synthesis kit. Expression quantification was performed using the Real-time PCR method using 2X SYBR Green master mix (Yekta Tajhiz, Iran), 1 µl of each forward and reverse primer, 1 µl of cDNA, and 4.5 µl of dH_2O on a RotorGene 6000 (Corbet Life Science, Australia). The Real-time program was 94 ℃ for 3 min, 95 ℃ for 10 s, 60 ℃ for 10 s, and 72 ℃ for 20 s for 40 cycles. U234 and Hprt were internal controls to normalize miR342 and mRNA levels, respectively. All applied primers are listed in Table 1.

Table 1. Primers used for Real-time PCR of miRNAs and genes

miR342-3p	RT primer	GTC GTA TGC AGA GCA GGG TCC GAG GTA TTC GCA CTG CAT ACG AC ACGGGT
	Forward primer	GGG TCT CAC ACA GAA ATC G
snoRNA234	RT primer	CGT ATG CAG AGC AGG GTC CGA GGT ATC CAT ACG CAT CGC ACT GCA TAC GAC CTC TCA G
	Forward primer	AGATTTAACAAAAATTCGTCAC
	Common Reverse primer	GAG CAG GGT CCG AGG T
ID4	Forward primer	ATGGATGGCCAGGTGTGC
	Reverse primer	CGTACGGTGAATGCTCGTGA
Bcl2l1	Forward primer	CTTCTGAGCTGCCTACCAGG
	Reverse primer	TCCAAAGCCAAGATAAGGTTATTCA
Mcl1	Forward primer	GGGGCAGGATTGTGACTCTTA
	Reverse primer	GAACTCCACAAACCCATCCCAG
Hprt	Forward primer	CTGGTGAAAAGGACCTCTCGAAG
	Reverse primer	CCAGTTTCACTAATGACACAAACG

Statistical analysis

All results are presented as the mean ± SD (*p<0.05, ** p<0.01, and *** p<0.001). For *in vitro* and *in vivo* experiments, the student's T-test was employed with GraphPad Prism 6.0 software, and Real-time PCR data were analyzed statistically using REST 2009 software.

Results

Chemical transfection of Hek-LentiX cells with PEI

Based on the GEO database, the expression of miR342-3p showed a significant reduction in the 4T1 cell line compared to non-metastatic breast cancer cells (GSE43483, Fig. 1A). The target scan database and KEGG signaling pathway demonstrated that this miRNA is conserved among animals and is involved in the growth, cell cycle, and apoptosis processes.

In this study, we have used the Hek-LentiX cell to package lentivirus particles, the best cell line for the expression of recombinant genes. Hek-LentiX cells were directly transfected with miR342 plasmid to optimize the purified miR342 plasmid and to reach the suitable PEI: DNA ratio for virus production. These cells were transfected at the 80% confluency and with 2:1 ratio of PEI: DNA. About 18 hours after transfection, the medium was changed to the complete medium, and 48 hours after transfection, the GFP-positive cells could be detected using a fluorescent microscope (Fig. 1B up); however, 96 hours of incubation led to cell apoptosis because of miR342 expression.

Transfection of Hek-LentiX cells with pMD2G, psPAX, pCDH, and pCDH-miR342 plasmids for virus production

Hek-LentiX cells were divided into control and treatment groups. Virus packaging was performed with pMD2G, psPAX, and scramble plasmids in the control group, and with pMD2G, psPAX, and miR342 plasmids in the treatment group. 72 hours after transfection, the GFP-positive cell population could be detected in both groups, indicative of transferring pCDH and pCDH-miR342 (Fig. 1C). Conditioned media containing the virus was collected every 12 hours for 3-5 days. Next, Hek-LentiX and 4T1 cells were seeded in 96-well plates to determine the quality and quantity of produced viruses. High GFP expression in Hek-LentiX after 96 hours indicated the high quality of produced viruses (Fig. 1B down); however, low transduction of 4T1 cells determined that these cells needed a virus booster (data not shown).

Antibiotic selection of 4T1 cells after transduction

Since we needed a stable population of miR342-expressing cells, antibiotic selection with puromycin was used to eliminate the antibiotic-sensitive cells (Fig. 1D). Flow cytometry analysis showed 95% GFP-positive cells after the selection (Fig. 1E). To ensure the miRNA expression, Real-time PCR was performed on 4T1 cells before and after transduction with miR342. Our results confirmed the overexpression of this miRNA in the miR342-transduced cells compared to scramble-transduced cells (Data not shown).

Figure 1

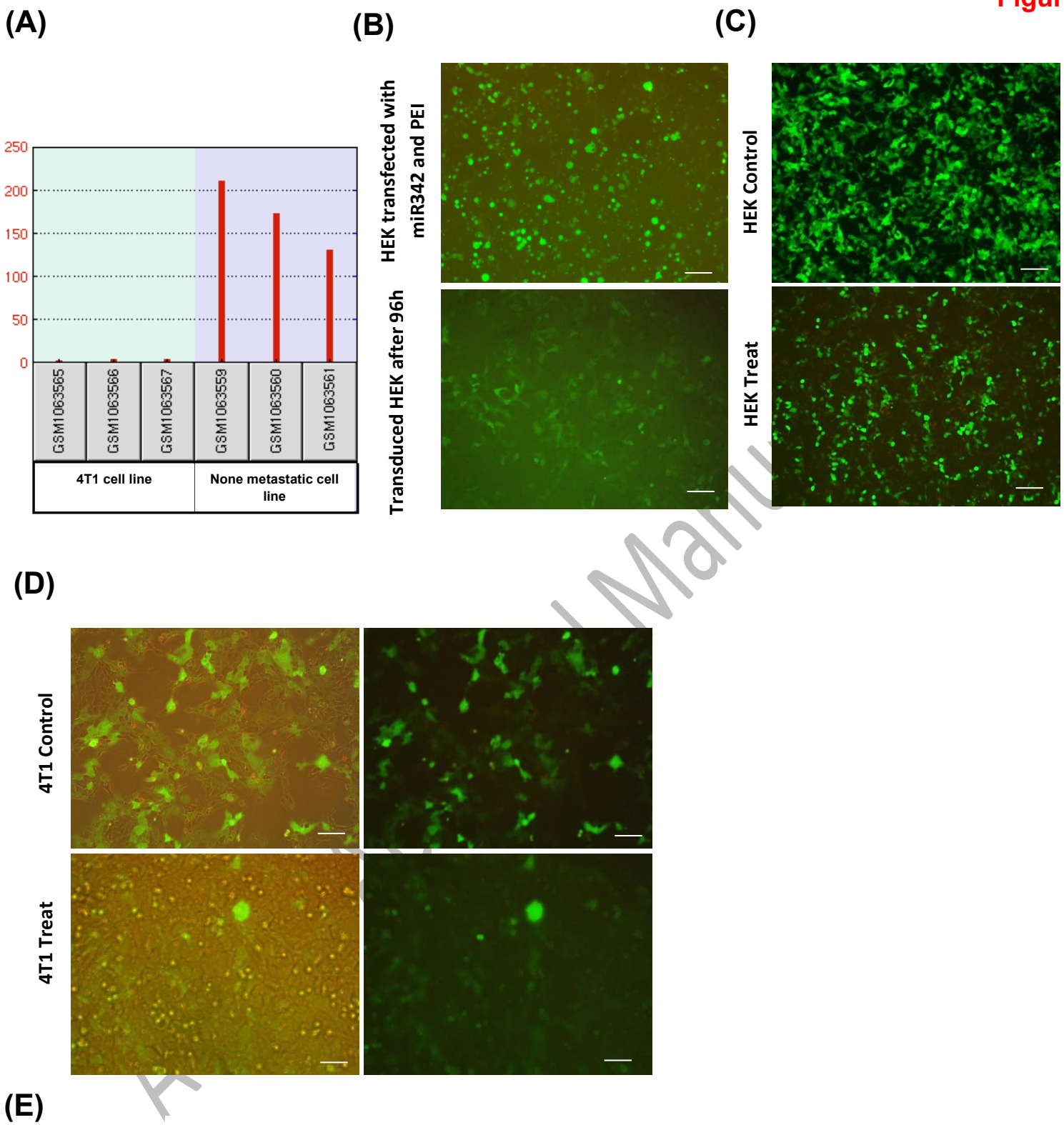
(A)
250
200
150
100
50
0
GSM1063565
GSM1063566
GSM1063567
GSM1063559
GSM1063560
GSM1063561
4T1 cell line
None metastatic cell line
(B)
HEK transfected with miR342 and PEI
Transduced HEK after 96h
(C)
HEK Control
HEK Treat
(D)
4T1 Control
4T1 Treat
(E)
4T1
miR342- 4T1
SSC-H
FL1-H:: GFP
GFP Positive
0.321%
GFP Positive
94.6%

Effect of miR342 on the viability and colony-forming ability of 4T1 cells

MTT assay was used to determine the effect of miR342 expression on the viability of 4T1 cells. Our data demonstrated no difference between the viability of the control and treatment groups within 24 hours. However, after 48 to 96 hours, cell viability was reduced by about 30-50% ($p<0.01$) in the treatment group compared to the control group (Fig 2A). This data shows that miR342 reduces cell viability, but the practical expression of miR342 starts after 48 hours. Colony formation assay outlines the ability of single cells to proliferate and make a colony. For this, about 100 cells were seeded in each well of the 6-well plate, and after 10 days, the number of colonies was counted, and their surface area was measured. Our data showed that the number of colonies in the treatment group was reduced by 50% compared to the control group (Fig. 2B, D). Also, Image J software measured the colony surface area in both groups. It was shown that (Fig. 2C, E) the colony size in the treatment group was reduced significantly compared to the control group.

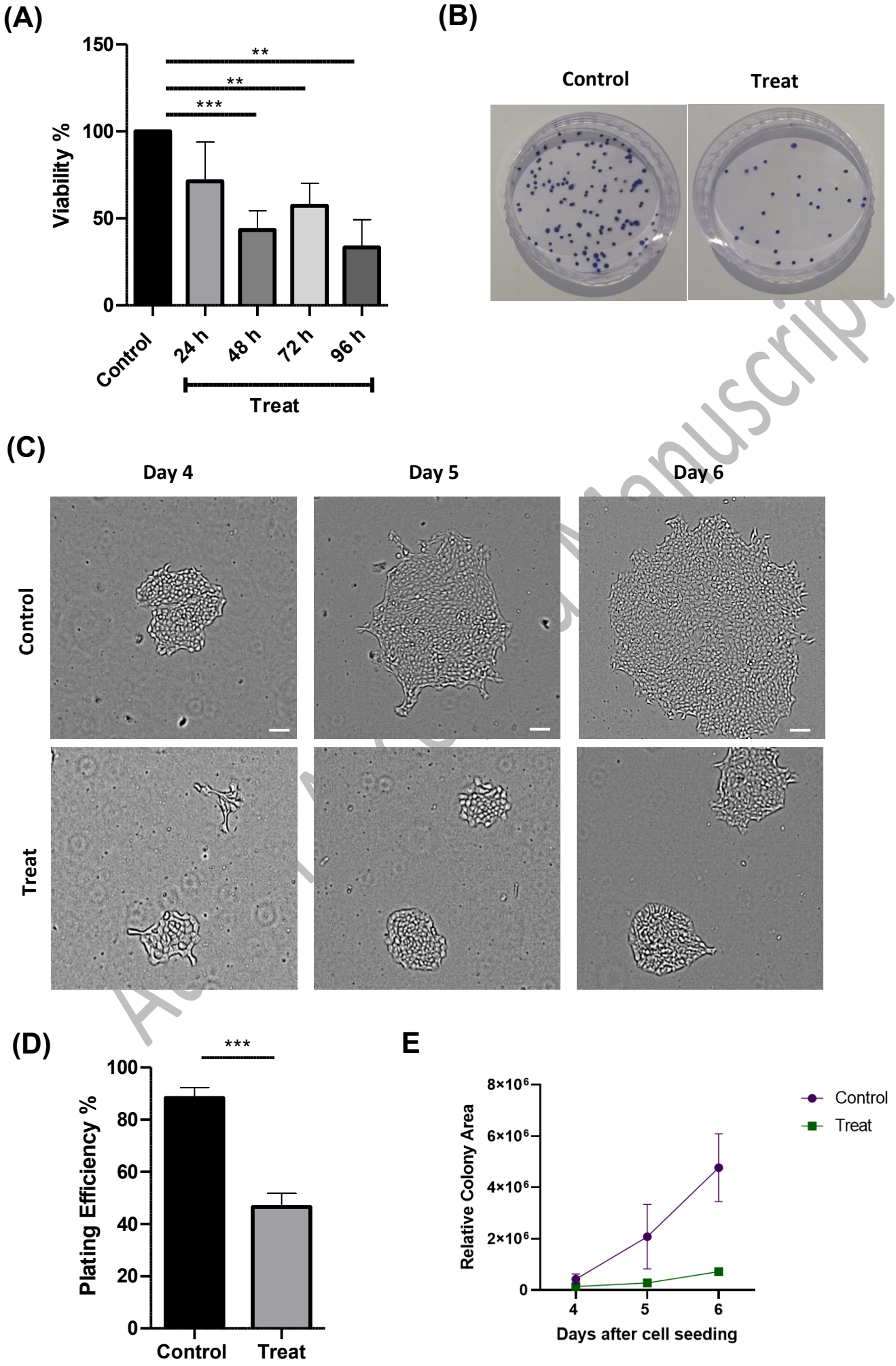

Apoptotic effect of miR342 on 4T1 cells

Apoptotic cells reveal phosphatidylserine on their surface, which can react with the annexin protein, so annexin positivity indicates the apoptotic cell population. Therefore, to determine the apoptosis-inducing effects of miR342, the 4T1 cells with the stable expression of miR342 were cultured in 6-well plates, and after 72 hours, they were analyzed with annexin/7-AAD and cell cycle assays. Flow cytometry analysis revealed that in the treatment group, the apoptosis rate was increased 1.6 times compared to the control group (Fig. 3A). This data was confirmed with 6.3 times increment of the sub-G1 population in the cell cycle of the treatment group, which defines the apoptosis rate (Fig. 3A).

Effect of miR342 on the migration behavior of 4T1 cells

A wound-healing assay was employed to evaluate the effect of miR342 on the migration behavior of 4T1 cells. The gap area was measured using Image J software between 0-72 hours after scratch formation. The percentage of wound healing in the treatment group after 24, 48, and 72 hours demonstrated a significant reduction compared to the control group (Fig. 3B, C). This confirms that miR342 can reduce the invasion characteristic of the 4T1 line as a robust metastatic cell line.

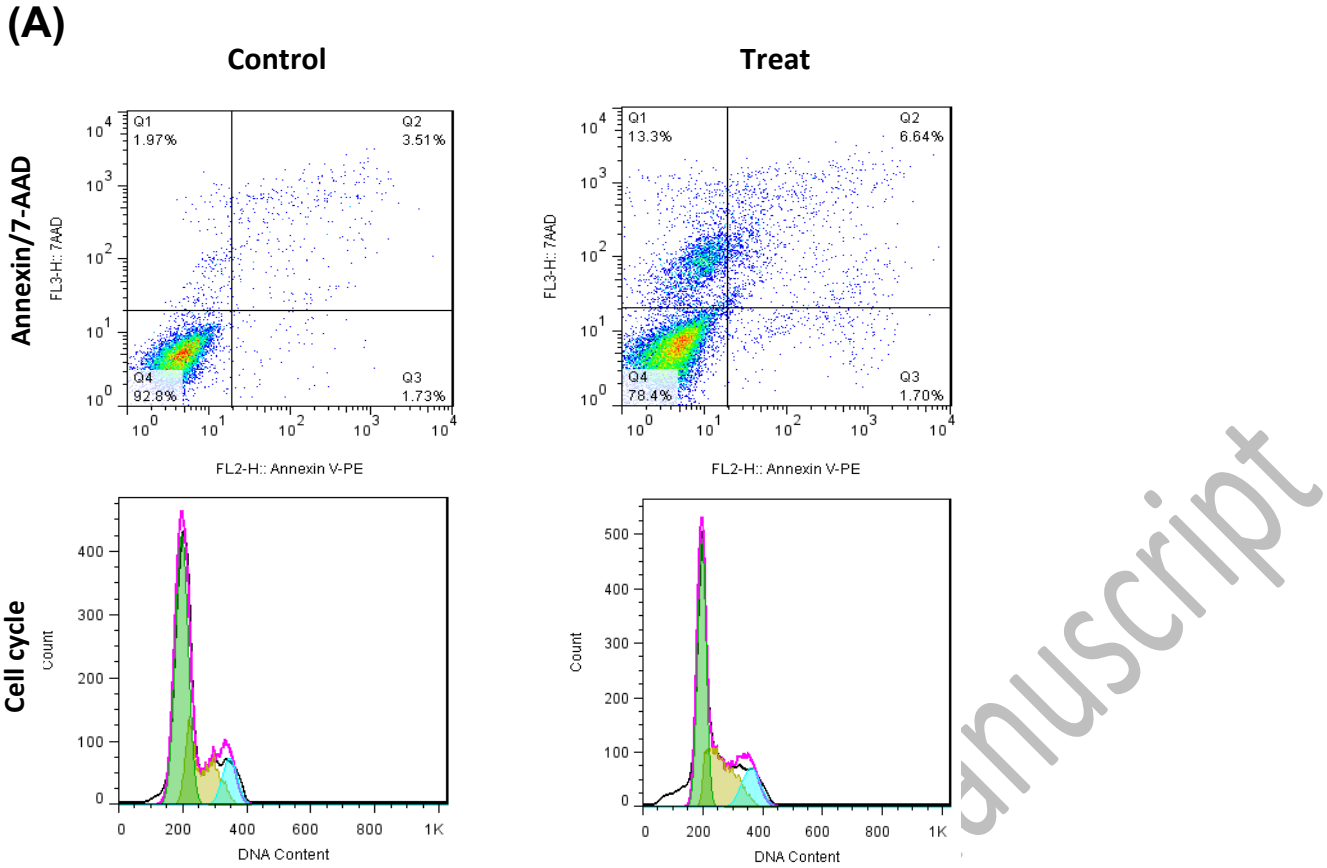

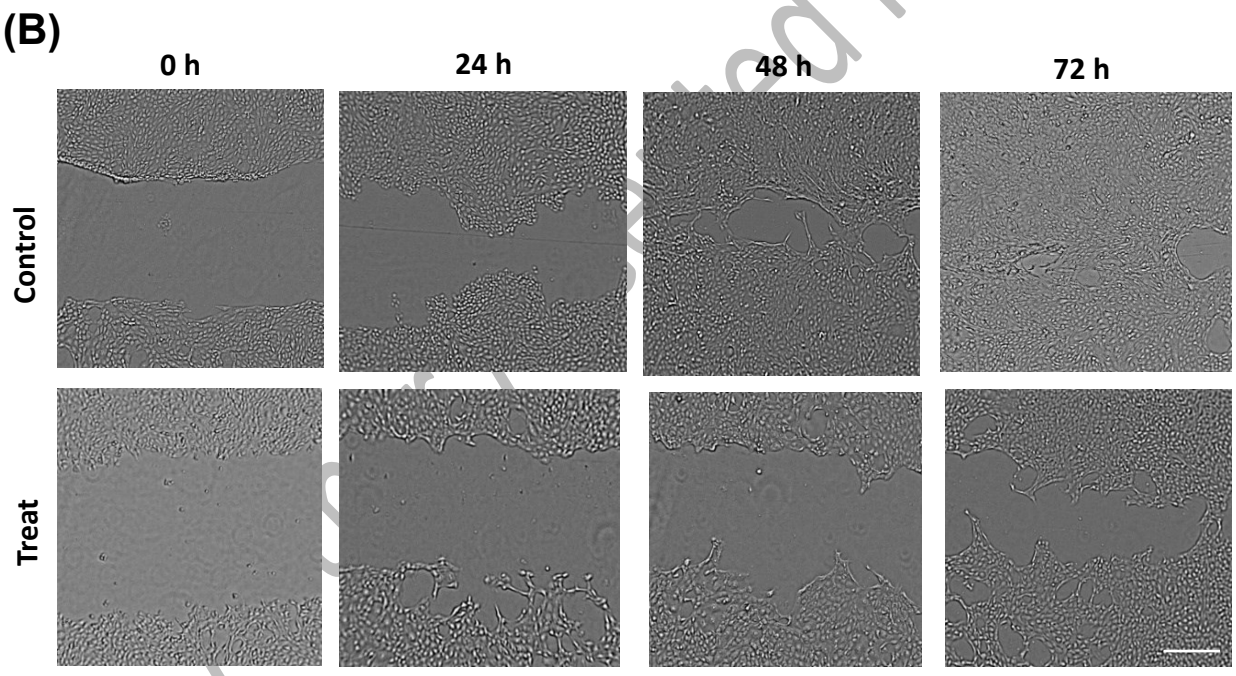

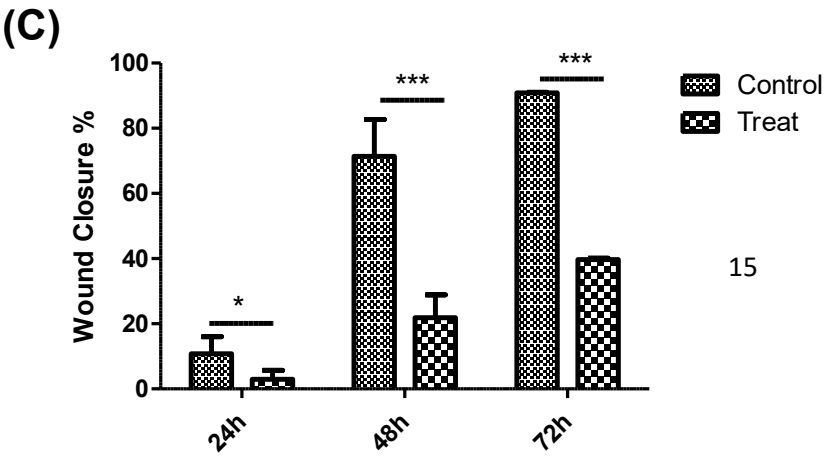

Effect of miR342 on the tumor growth in the mice model

In the last step, we evaluated the ability of miR342-transduced cells for tumor formation in an animal model. Therefore, miR342-transduced and scrambled cells were transplanted subcutaneously into Balb-C mice, and tumor growth was monitored daily for 30 days. The tumor growth in the treatment group showed a decreasing trend during these 30 days in a way that on the last day average tumor volume in this group reduced to 30% of the control group (Fig. 4A, B). On the last day, tumors were removed and weighed, with 2 times reduced tumor weight in the treatment group compared to the control group (Fig. 4C). It should be noted that no reduction in body weight was observed in the treatment group. Real-time PCR confirmed the continuous overexpression of miR342 in the treatment group 30 days after cell transplantation (Fig. 4D). The H&E staining and pathology scoring of tumor slides proved that the mitotic count from 15/10HPF in the control tumor was reduced to 8/10HPF in the treatment group (Fig. 4E). Also, the nuclear polymorphism of grade III in the control tumor was reduced to grade II in the treated tumor. The overall grade of the treatment tumor was diagnosed near II compared to grade III of the control tumor. These data prove that miR342 effectively suppresses tumor growth and reduces tumor grade.

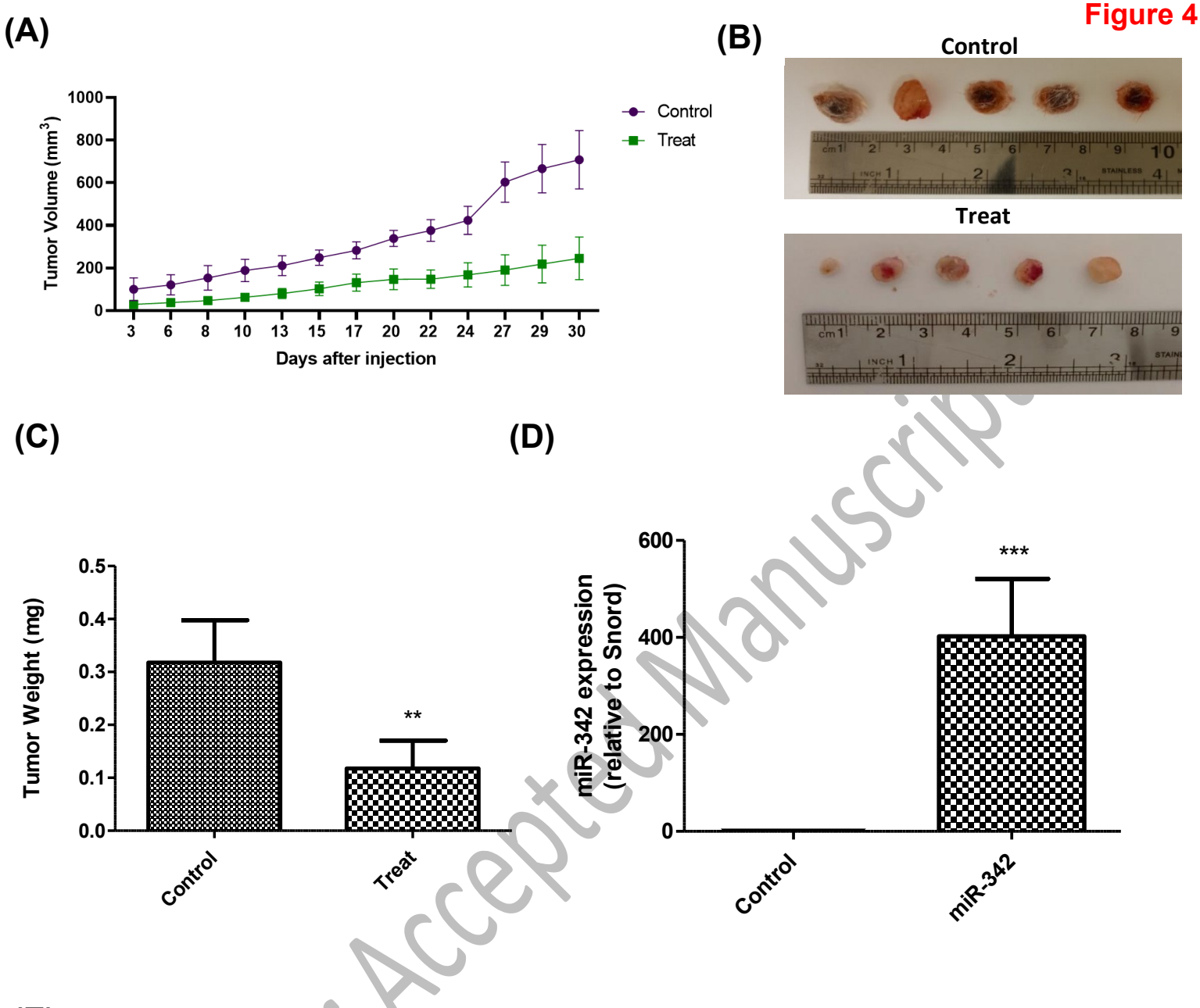

Effect of miR342 on the expression of target genes and proteins of tumor tissue

For the last step, the expression of some direct and indirect target genes and proteins of miR342 was assessed in the tumor tissues. The expression of two direct target genes, Bcl2l1 and Mcl1, as pro-apoptotic factors were significantly reduced in the tumors of the treatment group (Fig. 5A). Based on the target scan analysis, ID4 is one of the target genes of miR342, whose expression was reduced significantly in the treatment group (Fig. 5A). VEGF is a protein involved in angiogenesis. The immunostaining assay showed that expression of this protein was reduced in the treatment group compared to the control group. Also, the expression of Bax protein as an apoptotic factor increased in the treatment group, accompanied by a slight decrease in the expression of Bcl2 as an anti-apoptotic factor (Fig. 5B). These data prove the apoptotic and anti-angiogenic effect of miR342 on TNBC *in vivo*.

Figure 5

(A)

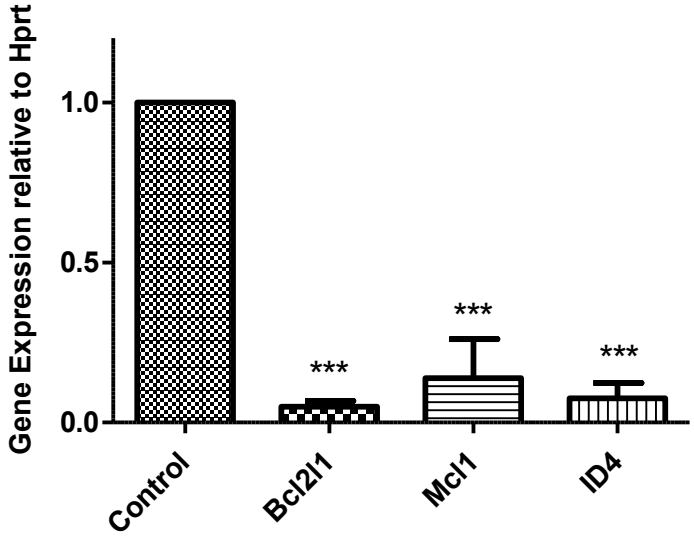

(B)

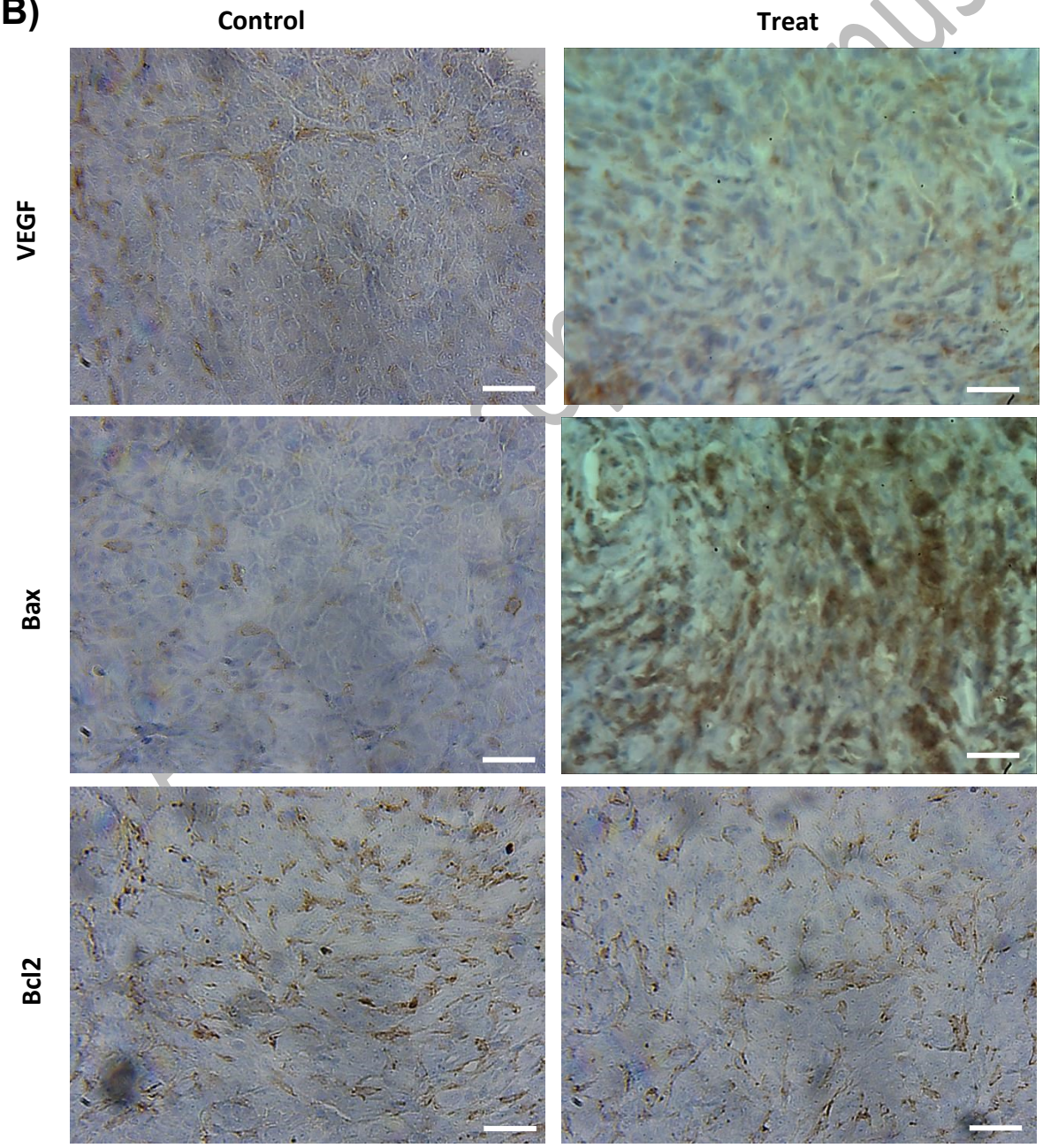

Discussion

Here we have studied the role of miR342 on mice triple-negative breast cancer *in vitro* and *in vivo*. It is known that expression of this miRNA is reduced in ovary cancer[15], glioblastoma[14], liver[9], and lung cancers[10], indicative of its essential role in tumorigenesis. Also, it was found that the expression of this miRNA is reduced by 10-fold in human breast cancer cell lines, including MDA-MB-231, MDA-MB-436, SK-BR-3, and CAMA-1[12]. The GEO database reported the reduced expression of miR342 in metastatic 4T1 cells compared to non-metastatic cells (GSE43483). Viral and non-viral transfection systems are used to deliver the interest miRNA into the cells. Virus-based methods mostly employ retro and lentiviruses with a high transfection efficacy, although accompanied by high immunogenicity; however, the safety of non-viral vectors is higher but with lower efficiency.[16] Chemical delivery systems mostly use polymeric lipid carriers. High molecular polyethyleneimine (PEI) as a protonated polymer exert low cell toxicity and seem to be a proper candidate for the delivery of miRNAs. Previously, miR33a and miR145 were successfully delivered to colon cancer cells via the PEI-based system in the mice model.[17] We first tried different PEI:DNA ratios to transfect 4T1 cells in the present study. However, this method could not efficiently deliver miR342 to these cells. Therefore, we have used lentiviral vectors for plasmid transfection. Evaluation of GFP expression via fluorescent microscope and flow cytometry validated the high rate of cell transfection with this method. Also, the overexpression of this miRNA in the transduced-4T1 cells was proved with Real-time PCR.

For the first step, the effect of miR342 on 4T1 cell viability was assessed. There was no significant decrease in the percentage of viable cells in 24 hours; however, 48 hours after cell seeding, a significant viability reduction was detected in the miR342-transduced cells. In line with our result, a study in 2020 showed that overexpression of miR342 in MDA-MB-436 and CAMA-1 breast cancer cell lines reduced viability in a time-dependent manner.[12] Also, excess miRNA expression in the hepatocellular carcinoma cells induced viability reduction 72 and 96 hours after cell seeding.[9] Next, the colony formation assay proved that miR342 overexpression in 4T1 cells alleviates the clonogenic ability of single cells. This assay determines the unlimited proliferation of a single cell to make a colony of at least 50 cells. Previous data also showed that this miRNA reduces the colony-forming capacity of MDA-MB-436 and CAMA-1 cell lines in a significant manner.[12] The reduced cell viability in the miR342 transduced-4T1 cells could result from apoptosis induction or cell cycle arrest. Our data showed the augmentation of the annexin-positive cells and an increase in the sub-G1 population in the treatment group, both indicative of apoptosis induction. In agreement with this, the apoptotic effect of miR342 on breast cancer, non-small cell lung cancer (NSCLC), and chronic myeloid leukemia (CML) was proved formerly.[10, 12, 18] Next, we assessed the effect of this miRNA on cancer cell migration, and our data confirmed that miR342 could prohibit the migration ability of 4T1 cells *in vitro*. In line with this data, the transwell assay detected the inhibitory effect of this miRNA on the invasive

behavior of ovarian cancer cells.[15] Downregulation of FOXQ1 as a target of miR342 appears to result in reduced invasiveness because this protein plays a decisive role in the EMT (epithelial to mesenchymal transition) property of different cancers. Moreover, miR342 could inhibit the migration of melanoma cancer cells via direct suppression of ZEB1, a zinc finger family member whose upregulation is reported in many types of cancers.[19]

Here we have also evaluated the tumorigenic properties of miR342-transduced 4T1 cells in a mouse model. Our data showed that during the 30 days follow-up after tumor induction, a significant reduction trend in tumor volumes between the treatment and control groups was detectable. Also, the tumor weight of the treatment group on the last day of follow-up showed a significant reduction compared to the control group. In line with our results, the inhibitory effect of miR342 on the tumor growth of mice bearing chronic myeloid leukemia model after 14 days was reported, confirming that this miRNA might be a critical target for the treatment of this cancer.[18] In addition, slower tumor growth of NSCLC in Balb/c models was detected after 42 days in mice injected with the miR342 mimics every 7 days.[10] Moreover, a four-week track of tumor growth in a xenograft ovary cancer model also revealed the prohibitory effect of miR342 on this cancer.[15]

In our study, assessment of miR342 expression after tumor removal at day 30 confirmed the prolonged expression of this miRNA *in vivo*. Tumor grades are determined based on the microscopic appearance of tumor cells. Our study's pathology diagnosis based on H&E staining of tumor slides demonstrated the reduced mitotic index, lower nuclear polymorphism, and overall reduced tumor grade in the treated tumor.

Furthermore, gene expression analysis of miR342-treated tumor tissues demonstrated the reduced expression of Bcl2l1, Mcl1, and ID4 compared to the control tumor. Bcl2l1 is a member of the Bcl2 family with anti-apoptotic properties, which can also lead to the anchorage-independent growth of cancer cells,[20] and inhibition of this gene in triple-negative breast cancer has resulted in the suppression of metastasis.[21] Formerly, a strong correlation between the overexpression of Bcl2l1 and higher grades of breast cancer and metastasis was reported.[22] In agreement with our results, it was demonstrated previously that miR342 directly targets the 3′UTR of Bcl2l1 mRNA in glioblastoma cancer.[14]

Also, Mcl1, a survival factor from the Bcl2 family, might be a direct or indirect target of miR342.[14] Mcl1 inhibitors can boost the efficacy of conventional treatments since this molecule is highly expressed in breast cancer,[23] especially the triple-negative type is highly dependent on this protein.[24] Interestingly, Mcl1 overexpression in breast cancer is more common than that of Bcl2 and Bcl2l1.[25] Therefore, targeted treatments leading to reduced expression of this gene could be highly important in reducing TNBC tumor growth. ID4 (inhibitor of DNA binding) is a transcription factor whose over-expression is reported in many types of cancer, including breast, lung, and hepatocellular cancers. It was demonstrated that ID4, as the direct target of miR342, is

one of the essential players regulating cell proliferation and invasion.[26,27] Moreover, it was reported that miR342 could affect BRCA1 expression indirectly via direct inhibition of ID4 in MDA-MB-231 triple-negative breast cancer cells.[28] In fact, ID4 is an oncogene whose inhibitory role on the regulation of BRCA1 tumor suppressor factor was detected before.[29]

We have also assessed the expression of some direct and indirect targets of miR342 on protein levels. The immunohistochemistry of tumor tissue indicated the decreasing expression of Bcl2 protein concomitant with the increased expression of Bax in the miR342-overexpressed group. Bcl2 and Bax proteins belong to the Bcl2 family, in which Bcl2 is an anti-apoptotic and Bax is a pro-apoptotic factor. Most of the time, induction of apoptosis would lead to the decreased ratio of Bcl2/Bax. In line with our result, it was shown with luciferase assay that Bcl2 is a direct target of miR342 in the NSCLC cells, and the miR342-transfected tumor tissues demonstrated decreased expression of Bcl2 protein.[10] Also, the decreased ratio of Bcl2/Bax in breast cancer and hepatocellular cells transfected with miR342 mimics was reported, indicating the tumor suppressor role for this miRNA.[9, 12]

Additionally, the IHC result showed the decreased expression of VEGF in miR342-transfected tumors compared to the control group. VEGF is a pro-angiogenic factor which is essential for the formation of new vessels in the tumor tissue. A previous study reported the inductive effect of ID4 on VEGF production in breast cancer cells. Therefore, it seemed that miR342 indirectly suppressed the expression of VEGF due to the negative regulation of ID4.[30]

Conclusion

To conclude, our *in vitro* results showed that miR342 could reduce cell viability and invasive behavior of TNBC 4T1 cells. Also, this miRNA could prohibit tumor progression and angiogenesis by suppressing the expression of anti-apoptotic and angiogenic factors, including Bcl2, Mcl1, and VEGF. Our data support the idea that this miRNA might be a potential therapeutic target to be used alone or in combination with chemotherapy to treat TNBC with limited therapeutic options. In this way, the tumor cells are attacked in a multipurpose approach through the intervention of different signaling pathways, which can synergically lead to the eradication of breast cancer. However, it should be noted that for clinical applications, miRNA transfer to the tumor site would be accomplished via systemic administration using a proper delivery system. This could open the way for miRNA mimics to be used along with chemotherapy as an adjuvant therapy to stop the progression of TNBC.

Funding sources

This project was funded by the University of Tehran, Faculty of Biology.

Ethical statement

Animal experiments were performed in line with the principles of the declaration of Helsinki. Approval was granted by the faculty of biology at the University of Tehran.

Competing interests

The authors declare no competing financial interests.

Author contributions

FA and EA contributed to the study conception and design. Material preparation, data collection, and analysis were performed by ZA. FS performed the Real-time PCR and coached ZA through the research. The first draft of the manuscript was written by FA, and all authors commented on previous versions of the manuscript. All authors read and approved the final manuscript.

Research Highlights

What is the current knowledge?

• Human triple negative breast cancer cells with higher expression of miR342 demonstrated more sensitivity to the chemotherapy

• miR342 inhibited the proliferation of human breast cancer cells *in vitro*

• The therapeutic effect of miR342 overexpression on the triple negative breast tumor in the animal model was not investigated

What is new here?

• miR342 inhibited the proliferation and migration of mice triple negative breast cancer cells *in vitro*

• miR342 reduced the progression rate and mitotic index of triple negative breast tumors in the mice model

• The expression of anti-apoptotic target genes of miR342, including Bcl2l1, Mcl1, ID4, and VEGF was decreased in the tumor tissue due to the miR342 overexpression

• The expression of pro-apoptotic Bax protein was increased in the tumor tissue due to the miR342 overexpression

- **References**

1. Malorni L, Shetty PB, De Angelis C, Hilsenbeck S, Rimawi MF, Elledge R*, et al.* Clinical and biologic features of triple-negative breast cancers in a large cohort of patients with long-term follow-up. *Breast Cancer Res Treat* **2012**; 136: 795-804. doi: 10.1007/s10549-012-2315-y.
2. Szymiczek A, Lone A, Akbari MR. Molecular intrinsic versus clinical subtyping in breast cancer: A comprehensive review. *Clin Genet* **2021**; 99: 613-37. doi: 10.1111/cge.13900.
3. O'Reilly EA, Gubbins L, Sharma S, Tully R, Guang MH, Weiner-Gorzel K*, et al.* The fate of chemoresistance in triple negative breast cancer (TNBC). *BBA Clin* **2015**; 3: 257-75. doi: 10.1016/j.bbacli.2015.03.003.
4. Ding L, Gu H, Xiong X, Ao H, Cao J, Lin W*, et al.* MicroRNAs Involved in Carcinogenesis, Prognosis, Therapeutic Resistance and Applications in Human Triple-Negative Breast Cancer. *Cells* **2019**; 8. doi: 10.3390/cells8121492.
5. Deng X, Cao M, Zhang J, Hu K, Yin Z, Zhou Z*, et al.* Hyaluronic acid-chitosan nanoparticles for co-delivery of MiR-34a and doxorubicin in therapy against triple negative breast cancer. *Biomaterials* **2014**; 35: 4333-44. doi: 10.1016/j.biomaterials.2014.02.006.
6. Han G, Bai X, Jiang H, He Q. MicroRNA-598 inhibits the growth of triple negative breast cancer cells by targeting JAG1. *Exp Ther Med* **2021**; 21: 235. doi: 10.3892/etm.2021.9666.
7. Fan C, Liu N, Zheng D, Du J, Wang K. MicroRNA-206 inhibits metastasis of triple-negative breast cancer by targeting transmembrane 4 L6 family member 1. *Cancer Manag Res* **2019**; 11: 6755-64. doi: 10.2147/CMAR.S199027.
8. Dong Y, Liu Y, Jiang A, Li R, Yin M, Wang Y. MicroRNA-335 suppresses the proliferation, migration, and invasion of breast cancer cells by targeting EphA4. *Mol Cell Biochem* **2018**; 439: 95-104. doi: 10.1007/s11010-017-3139-1.
9. Lu C, Jia S, Zhao S, Shao X. MiR-342 regulates cell proliferation and apoptosis in hepatocellular carcinoma through Wnt/beta-catenin signaling pathway. *Cancer Biomark* **2019**; 25: 115-26. doi: 10.3233/CBM-192399.
10. Chen Z, Ying J, Shang W, Ding D, Guo M, Wang H. miR-342-3p Regulates the Proliferation and Apoptosis of NSCLC Cells by Targeting BCL-2. *Technol Cancer Res Treat* **2021**; 20: 15330338211041193. doi: 10.1177/15330338211041193.
11. Ma T, Zhang J, Wu J, Tang J. [Effect of miR-342-3p on chemotherapy sensitivity in triple-negative breast cancer]. *Zhong Nan Da Xue Xue Bao Yi Xue Ban* **2014**; 39: 488-95. doi: 10.3969/j.issn.1672-7347.2014.05.009.
12. Liu C, Xing H, Luo X, Wang Y. MicroRNA-342 targets Cofilin 1 to suppress the growth, migration and invasion of human breast cancer cells. *Arch Biochem Biophys* **2020**; 687: 108385. doi: 10.1016/j.abb.2020.108385.
13. Romero-Cordoba SL, Rodriguez-Cuevas S, Bautista-Pina V, Maffuz-Aziz A, D'Ippolito E, Cosentino G*, et al.* Loss of function of miR-342-3p results in MCT1 over-expression and contributes to oncogenic metabolic reprogramming in triple negative breast cancer. *Sci Rep* **2018**; 8: 12252. doi: 10.1038/s41598-018-29708-9.
14. Ghaemi S, Arefian E, Rezazadeh Valojerdi R, Soleimani M, Moradimotlagh A, Jamshidi Adegani F. Inhibiting the expression of anti-apoptotic genes BCL2L1 and MCL1, and apoptosis induction in glioblastoma cells by microRNA-342. *Biomed Pharmacother* **2020**; 121: 109641. doi: 10.1016/j.biopha.2019.109641.
15. Wang C, Zhang W, Xing S, Wang Z, Wang J, Qu J. MiR-342-3p inhibits cell migration and invasion through suppressing forkhead box protein Q1 in ovarian carcinoma. *Anticancer Drugs* **2019**; 30: 917-24. doi: 10.1097/CAD.0000000000000801.

16. Yang N. An overview of viral and nonviral delivery systems for microRNA. *Int J Pharm Investig* **2015**; 5: 179-81. doi: 10.4103/2230-973X.167646.
17. Ibrahim AF, Weirauch U, Thomas M, Grunweller A, Hartmann RK, Aigner A. MicroRNA replacement therapy for miR-145 and miR-33a is efficacious in a model of colon carcinoma. *Cancer Res* **2011**; 71: 5214-24. doi: 10.1158/0008-5472.CAN-10-4645.
18. Wu YY, Lai HF, Huang TC, Chen YG, Ye RH, Chang PY*, et al.* Aberrantly reduced expression of miR-342-5p contributes to CCND1-associated chronic myeloid leukemia progression and imatinib resistance. *Cell Death Dis* **2021**; 12: 908. doi: 10.1038/s41419-021-04209-2.
19. Shi Q, He Q, Wei J. MicroRNA-342 Prohibits Proliferation and Invasion of Melanoma Cells by Directly Targeting Zinc-Finger E-Box-Binding Homeobox 1. *Oncol Res* **2018**; 26: 1447-55. doi: 10.3727/096504018X15193823766141.
20. Fernandez Y, Espana L, Manas S, Fabra A, Sierra A. Bcl-xL promotes metastasis of breast cancer cells by induction of cytokines resistance. *Cell Death Differ* **2000**; 7: 350-9. doi: 10.1038/sj.cdd.4400662.
21. Skov N, Alves CL, Ehmsen S, Ditzel HJ. Aurora Kinase A and Bcl-xL Inhibition Suppresses Metastasis in Triple-Negative Breast Cancer. *Int J Mol Sci* **2022**; 23. doi: 10.3390/ijms231710053.
22. Olopade OI, Adeyanju MO, Safa AR, Hagos F, Mick R, Thompson CB*, et al.* Overexpression of BCL-x protein in primary breast cancer is associated with high tumor grade and nodal metastases. *Cancer J Sci Am* **1997**; 3: 230-7. doi:
23. Winder ML, Campbell KJ. MCL-1 is a clinically targetable vulnerability in breast cancer. *Cell Cycle* **2022**; 21: 1439-55. doi: 10.1080/15384101.2022.2054096.
24. Campbell KJ, Dhayade S, Ferrari N, Sims AH, Johnson E, Mason SM*, et al.* MCL-1 is a prognostic indicator and drug target in breast cancer. *Cell Death Dis* **2018**; 9: 19. doi: 10.1038/s41419-017-0035-2.
25. Wang H, Guo M, Wei H, Chen Y. Targeting MCL-1 in cancer: current status and perspectives. *J Hematol Oncol* **2021**; 14: 67. doi: 10.1186/s13045-021-01079-1.
26. Patel D, Morton DJ, Carey J, Havrda MC, Chaudhary J. Inhibitor of differentiation 4 (ID4): From development to cancer. *Biochim Biophys Acta* **2015**; 1855: 92-103. doi: 10.1016/j.bbcan.2014.12.002.
27. Han X, Niu C, Zuo Z, Wang Y, Yao L, Sun L. MiR-342-3p inhibition promotes cell proliferation and invasion by directly targeting ID4 in pre-eclampsia. *J Obstet Gynaecol Res* **2020**; 46: 49-57. doi: 10.1111/jog.14150.
28. Crippa E, Lusa L, De Cecco L, Marchesi E, Calin GA, Radice P*, et al.* miR-342 regulates BRCA1 expression through modulation of ID4 in breast cancer. *PLoS One* **2014**; 9: e87039. doi: 10.1371/journal.pone.0087039.
29. Beger C, Pierce LN, Kruger M, Marcusson EG, Robbins JM, Welcsh P*, et al.* Identification of Id4 as a regulator of BRCA1 expression by using a ribozyme-library-based inverse genomics approach. *Proc Natl Acad Sci U S A* **2001**; 98: 130-5. doi: 10.1073/pnas.98.1.130.
30. Donzelli S, Milano E, Pruszko M, Sacconi A, Masciarelli S, Iosue I*, et al.* Expression of ID4 protein in breast cancer cells induces reprogramming of tumour-associated macrophages. *Breast Cancer Res* **2018**; 20: 59. doi: 10.1186/s13058-018-0990-2.

Figure Legends

Fig. 1. (**A**) Expression analysis of miR342 in 4T1 cells compared to none-metastatic cells based on GSE43483 data set. (**B**) Fluorescent image of Hek-LentiX cells 96 hours after direct transfection with miR342 using PEI in order to reach the suitable PEI:DNA ratio for virus production (Up). Fluorescent image of miR342-transduced Hek-LentiX cells 96 hours after transduction to validate virus authenticity (Down). (**C**) Fluorescent images of scramble (control) and miR342-transfected (Treat) Hek cells for lentivirus production. (**D**) Fluorescent images of scramble and miR342 transduced 4T1 cells after antibiotic selection (Scale bars equals 100 µm). **(E)** Flow cytometry histograms of 4T1 cells before and after transduction with miR342 to demonstrate GFP-positive cells

Fig. 2. (**A**) Viability diagram of scramble and miR342-transduced 4T1 cells, 24, 48, 72, and 96 hours after cell seeding, assessed with MTT assay. (**B**) Colony images of control and miR342-transduced 4T1 cells after 10 days. (**C**) Microscopic images of colonies of control and miR342-transduced 4T1 cells after 6 days (Scale bars equals 100 µm). (**D**) Plaiting efficiency of control and miR342-transduced 4T1 cells after 10 days. **E** Relative colony area of control and miR342-transduced 4T1 cells after 6 days (data are presented as mean $\pm$ SD, N=3, ** $p<0.01$ and *** $p<0.001$)

Fig. 3. (**A**) Detection of apoptosis using annexin/7AAD assay (Up) and cell cycle assay (Down) in control and miR342-transduced 4T1 cells. (**B**) Microscopic images of wound healing assay in control and miR342-transduced 4T1 cells. Photos are taken 24, 48, and 72 hours after scratch formation (Scale bars equals 200 µm). (**C**) Diagram of wound healing control and miR342-transduced 4T1 cells during 72 hours after scratch formation (data are presented as mean $\pm$ SD, *** $p<0.001$)

Fig. 4. *In vivo* effect of miR342 on tumor progression. (**A**) Tumor volume of control and miR342-transduced 4T1 cells during a 30-day follow-up in which a significant decrease in the tumor volume of the miR342 group compared to the control tumor can be observed. (**B**) Tumor size of control and miR342-transduced 4T1 cells at day 30. (**C**) Tumor weight of control and miR342-transduced 4T1 cells at day 30 (data are presented as mean $\pm$ SD, N=5, *** $p<0.001$). (**D**) Expression of miR342 at day 30 in the tumor tissue of control and miR342-transduced 4T1 cells. (**E**) The H & E staining of tumor sections of control and miR342-transduced 4T1 cells at day 30 (Scale bars equals 50 µm)

Fig. 5. (**A**) Real-time analysis of Bcl2l1, Mcl1, and ID4 genes from control and miR342-transduced tumor tissues (data are presented as mean $\pm$ SD and analyzed with REST, N=3, *** $p<0.001$). (**B**) Immunostaining for VEGF, Bcl2, and Bax proteins in the control and miR342-transduced tumor tissues (Scale bars equals 20 µm)